

# Supplementary Information to ‘Upward Electrical Discharges from Thunderstorms’,

P. Krehbiel, J. Rioussset, V. Pasko, R. Thomas, W. Rison, M. Stanley, H. Edens

## Electrodynamic Model

In this section we describe the electrodynamic model used to simulate the electrical activity of a storm and present additional details of using the model to investigate the occurrence of upward discharges. The model represents the storm charges as a vertical sequence of axially aligned, uniformly-charged cylindrical disks (Fig. S1), for which the electric field and potential profiles are calculated on the axis of the disks (Fig. 1b,c,e,f)<sup>31, 20</sup>. The altitudes, thicknesses, and radii of the charge disks are determined from three-dimensional mapping observations of the lightning activity in the storm being studied. The lightning observations are obtained by the New Mexico Tech Lightning Mapping Array (LMA), which accurately locates the sources of impulsive VHF radiation events in three spatial dimensions and time<sup>32</sup>. By analyzing the structure and development of individual lightning flashes, one is able to determine the location and polarity of the charge regions being penetrated by the discharge channels<sup>33, 34, 19</sup>. From an analysis of sequences of flashes, a picture is obtained of the charge structure of the storm involved in the lightning (Fig. 1a)<sup>14, 19</sup>.

For a normally-electrified storm, two currents are used to simulate the storm charging: a main current  $I_1$  between the mid-level negative (N) and upper positive (P) charge regions, and a second current  $I_2$  between the N and lower positive (LP) regions. An above-cloud, ohmic ‘screening’ current  $I_{sc}$  is calculated by the model to account for charge attracted to the cloud top from the conducting clear air above the storm. The current causes a layer of negative charge to form at the upper cloud boundary<sup>35</sup>, called the screening charge, that reduces the electric field above the cloud. The screening charge is represented by the uppermost disk in the model. The parameters of the charge regions used in this study are listed in Supplementary Table 1 and correspond to a July 31, 1999 storm<sup>14</sup> over Langmuir Laboratory in central New Mexico (3.2 km altitude above mean sea level).

Given the storm’s basic charge structure, the charging currents  $I_1$  and  $I_2$  are estimated by running the model in time and adjusting the currents to reproduce the observed average lightning rates<sup>31</sup>. Lightning is assumed to occur when the on-axis electric field exceeds a specified threshold value versus altitude. The threshold relation used in this study is  $E_{\text{thresh}} = E_0 e^{-z/z_0}$ , where  $E_0 = 302 \text{ kV m}^{-1}$  and the scale height  $z_0 = 8.4 \text{ km}$ . The  $E_{\text{thresh}}(z)$  values provide a good empirical estimate of the electric field at which lightning is initiated during in-cloud balloon-borne soundings<sup>36, 14, 37</sup>, with  $E_0$  being 40% higher than the breakeven electric field  $E_{be} = 216 \text{ kV m}^{-1}$  for energetic electron avalanches at sea level<sup>38</sup>. Lightning initiated between the N and P charge regions results in a normal intracloud (IC) discharge, while lightning initiated between the N and lower

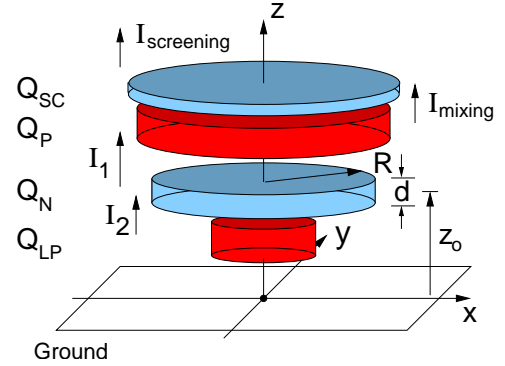


Figure S1. Cylindrical charge configuration of the electrodynamic model for a normally electrified storm, showing positive (red) and negative (blue) charge regions, and storm currents.

positive regions results in a negative cloud-to-ground ( $-CG$ ) discharge. IC discharges were nominally assumed to reduce the pre-flash storm charges by 50% of the lesser of charges  $Q_N$  and  $Q_P$ . CG discharges reduced  $Q_N$  and  $Q_{LP}$  by 50% each (assuming  $|Q_{LP}| < |Q_N|$ ), with the difference being the charge lowered to ground. The resulting changes in  $Q_N$  and  $Q_P$  were typically 30-40 C, comparable to values determined from lightning electric field change measurements<sup>39, 40, 41</sup>.

During the active stage of the July 31, 1999 storm, the storm produced 9 negative CG flashes and 30 IC flashes over a 14 min. time interval<sup>31</sup>. These average flashing rates are reproduced by the model for an upward charging current  $I_1 = 1.5$  A between the main dipolar (N, P) charge regions and a downward current  $I_2 = -0.1$  A into the lower positive charge (Fig. 1a). The average screening current to the cloud top was  $I_{sc} = 0.31$  A. To match the relative IC and CG rates, the criteria for CG discharges needed to be more stringent than that obtained from the threshold relation itself; this was accomplished by requiring the electric field  $E$  to exceed the breakdown threshold over a nominal vertical distance of 500 m before a CG flash was initiated (Fig. 1b).

Fig. S2 shows the variation of the storm charges and currents with time. During the first 400 s,  $I_1$  and  $I_2$  have the values that reproduce the average flashing rates. The storm behaves as a classic relaxation oscillator wherein the charging currents produce linear charge increases that are periodically relaxed by IC discharges and, less often, by CG discharges. The electric field and screening current above the cloud are predominantly upward-directed, corresponding to the downward transport of negative screening charge to the cloud top. This steadily drives the overall storm charge toward negative values until a  $-CG$  occurs (Fig. S2b). The sudden removal of negative charge causes the overall storm charge to revert to a positive value, at which point the cycle repeats. Actual storms are not as deterministic as the simple model, but exhibit similar basic behavior.

An important result of the model calculations has been that, when the cloud-top screening current and charge are accounted for, discharges are predicted to be initiated regularly between the upper positive (P) and negative screening (SC) charges in the uppermost part of the storm<sup>31, 42</sup>. Due to the imbalance in the magnitudes of the two charges, such breakdown would be expected to escape the cloud upward. The fact that upward jets do not occur in most storms leads to the conclusion that the screening charge is normally dissipated in some way, most likely by being mixed into the upper positive charge. Because atmospheric ions quickly become immobilized on cloud particles inside the storm<sup>43</sup>, such mixing would occur by convective overturning and turbulent processes or by a non-linear field-limiting process<sup>44, 45</sup>, rather than by steady ohmic conduction\*. The degree of mixing required to suppress the upper level breakdown is relatively strong; for the simulations of this study (including those of Fig. S2) the mixing was such that a non-replenished screening charge would be relaxed away exponentially with a time constant  $\tau_{mix} \simeq 60$  s.

For a given mixing rate, the model simulations indicate that upper level discharges can occur if the charging currents in the storm are increased. This is seen after  $t = 400$  s in Fig. S2. At that time both currents are doubled in magnitude, to  $I_1 = 3.0$  A and  $I_2 = -0.2$  A. This has the immediate effect of doubling the IC and CG flashing rates. In addition, over the next few minutes it also causes the net storm charge to drift toward an average positive value (Fig. S2b). The shift in net charge increases the vertical electric field in the upper part of the storm and leads to two upper-level discharges being triggered in the simulation. Electric field and potential profiles for the first of the indicated discharges, at  $t = 648$  s, have been presented in Fig. 1. The discharges would

---

\*Ion attachment causes electrical conduction currents to be negligibly small in clouds<sup>46</sup>; the model thus assumes the electrical conductivity to be zero inside the storm.

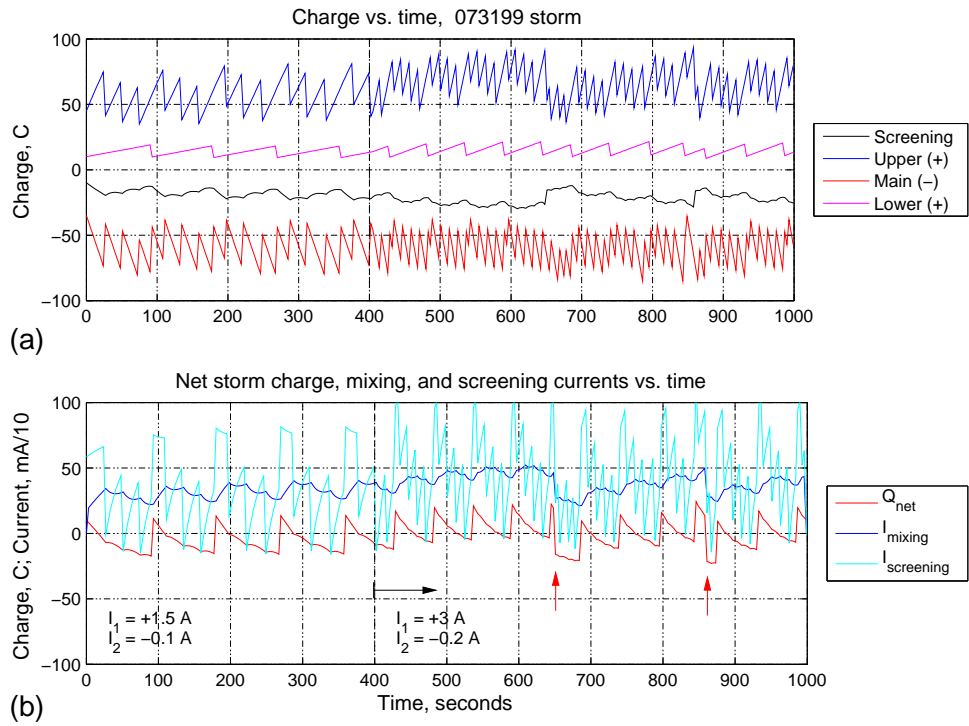


Figure S2: Model-calculated temporal variation of the storm charges and currents, showing the behavior that reproduces the average CG and IC flashing rates ( $t = 0$  to 400 s) and the effect of doubling the charging currents (starting at  $t = 400$  s). During the initial time interval, the screening current drives the overall storm charge  $Q_{net}$  toward negative values, while  $-CG$  discharges suddenly change the net charge to positive values (red line, panel b). The effect of increasing the charging current is to double the IC and CG flashing rates and to cause  $Q_{net}$  to develop a positive offset. The latter leads to the occurrence of upward discharges (red arrows), which cause changes in the screening charge, net charge, and mixing current (black line, panel a; red and blue lines, panel b).

transport positive charge upward (Fig. 1d) and are consistent with being of the blue jet variety. They are predicted to occur shortly after a CG discharge removes negative charge from the storm, which maximizes the storm's positive charge (Fig. S2b) and increases the vertical electric field in the upper part of the cloud (Fig. 1b).

The primary impetus for the onset of upper level discharges in the above simulation is the increased rate of occurrence of  $-CG$  discharges. This is indicated by the simulation of Fig. S3. Instead of increasing both charging currents,  $I_1$  remains constant at 1.5 A and only the lower positive charging current  $I_2$  is increased, in this case by a factor of three, to  $I_2 = -0.3$  A. This increases the  $-CG$  rate correspondingly while the IC rate remains essentially as before. As in Fig. S2, the net storm charge drifts to an average positive value and upper-level discharges are indicated to start several minutes later, again shortly after  $-CG$  discharges. The positive charge build-up results from the increased rate at which the CGs remove negative charge from the storm.

The above results indicate that BJs can occur during episodes of enhanced  $-CG$  activity or increased overall lightning rates. The simulation of Fig. S4 illustrates how reduced mixing of the screening charge can also result in BJs, at normal charging rates. In this simulation no mixing is assumed and the charging rates are left at their original value throughout the full time interval. Upward discharges are predicted to occur frequently, nearly as often as the  $-CG$  flashes, and without the storm needing to develop average net positive charge. Both features result from the

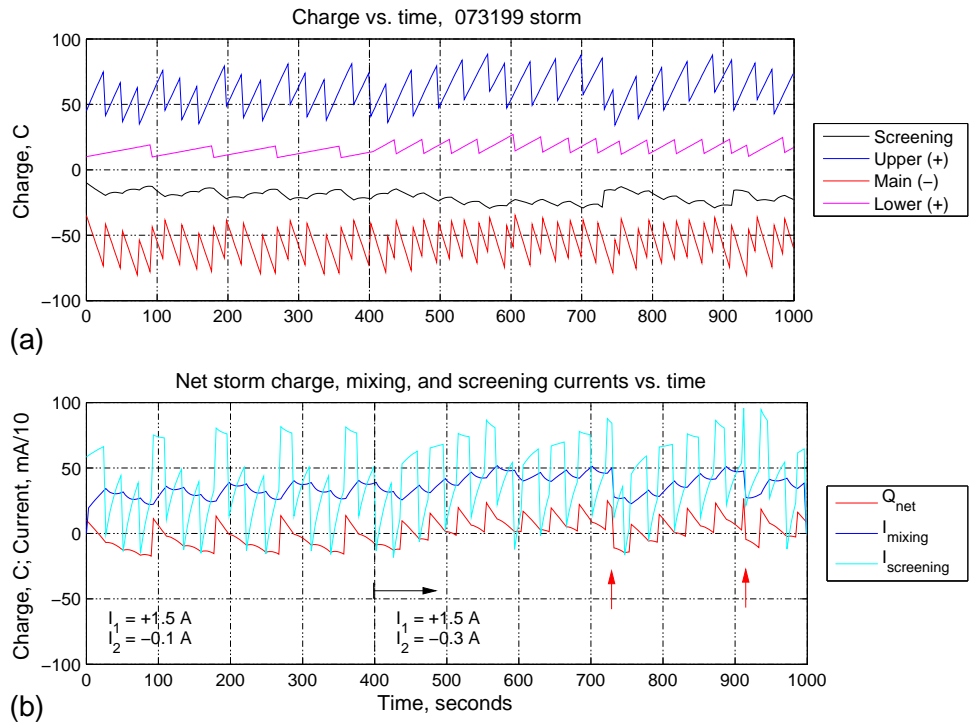


Figure S3: Same as Fig. S2, except that only the lower positive charging current  $I_2$  is increased, showing that the drift to net positive storm charge and the occurrence of upward discharges results from the increase in the  $-CG$  flashing rate.

electric field in the upper part of the cloud not being reduced by mixing. The upward discharges continue to be instigated by  $-CG$  flashes, but the increased favorability for such breakdown is reflected in some upward discharges occurring after an intervening IC flash and also during the initiating CG (Fig. S4b). The STEPS jet of Fig. 2 occurred in a relatively stratiform part of the storm and its occurrence may have benefited from reduced mixing.

In all simulations, the screening charge plays the same role in enhancing the electric field and triggering blue jet discharges as the lower positive charge plays in triggering  $-CG$  discharges.<sup>†</sup> While  $-CG$  discharges occur on their own, BJs require a charge-imbalancing precursor discharge (such as a  $-CG$ ) to make their triggering possible. In addition, rather than being triggered immediately during the precursor, as in Wilson's original suggestion<sup>16</sup>, the breakdown is often delayed 5 to 10 s or so after the initiating flash. In the simulations, the delay is manifested by the electric field not immediately exceeding the breakdown threshold after the CG, so that additional charging is required for the threshold to be reached. The basic reason for the time delay is more subtle than this, however, and has to do with a) the buildup of conditions favorable to blue jets occurring gradually with time, and b) the fact that, after each CG, the BJs have to compete with normal IC flashes to be the next discharge in the storm.<sup>‡</sup> That upward discharges compete with intracloud

<sup>†</sup>Rather than being initiated in the clear air above the cloud boundary and requiring an unrealistically strong electric field above the cloud for the discharge to propagate upward, as in the study by Sukhorukov *et al.*<sup>47</sup>, the above-cloud field is reduced by the screening charge (Fig. 1e) and the upward discharges are triggered in the cloud interior. The breakdown develops upward primarily by virtue of its channels being maintained at the high electric potential of the upper part of the storm (Fig. 1f). In addition, the upward breakdown is not restricted to be of negative polarity.

<sup>‡</sup>In particular, after each CG discharge the possibility exists of the next discharge being an IC flash between the N and P charge regions or upper-level breakdown between the P and negative screening charge (e.g., Fig. 1b). IC

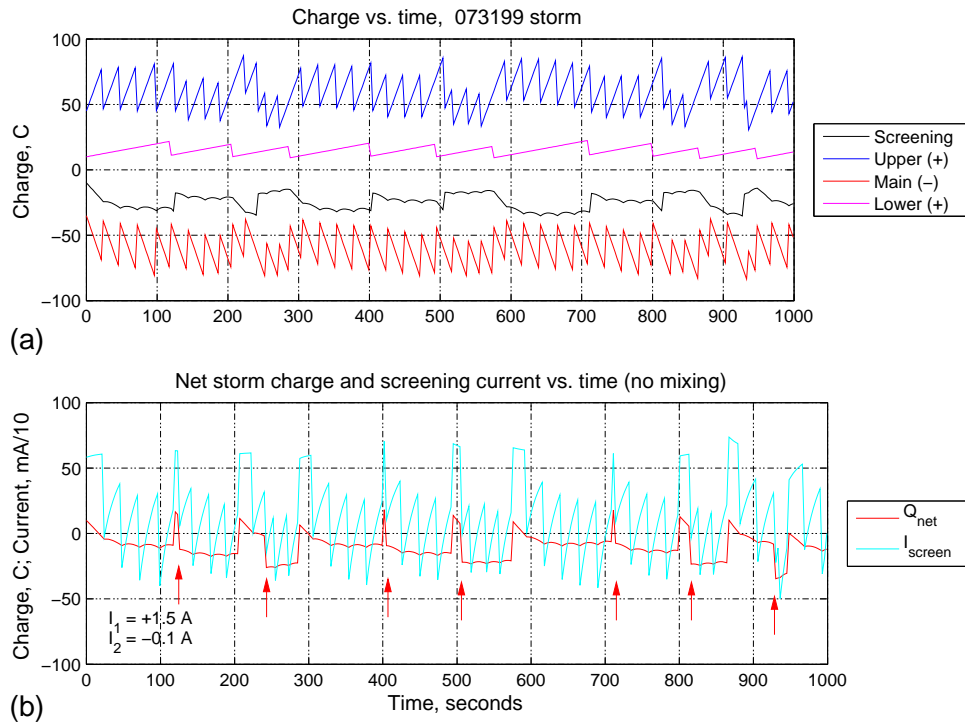


Figure S4: Same as Fig. S2, except that the screening charge is not mixed into the upper positive charge, showing the occurrence of a number of upward discharges are predicted to occur in the absence of such mixing. The charging currents remained constant throughout the full time interval. The storm does not need to develop a net positive charge for the upward discharges to be triggered, and upward discharges are predicted to occur almost as often as  $-CG$  discharges.

flashes, and are usually preempted by the ICs, is an important point seen both in the electrodynamic calculations and in the lightning simulations that has not been fully considered in previous studies<sup>22, 48, 13</sup>. Finally, BJ's are not precluded from being triggered immediately during the precursor discharge. This can happen either by chance or by the precursor removing a large fraction of the mid-level charge.

Assuming that upward discharges reduce the upper positive and screening charges by 50% each, analogous to  $CG$  discharges, the net upward charge transfer is typically +40-45 C, somewhat larger in magnitude than the  $-CG$  charge amounts.

## Supporting Discussion

The electrodynamic simulations suggest that blue jet discharges occur in parts of a storm where mixing of the screening charge is reduced, and/or during episodes of enhanced  $CG$  activity in a storm. Both scenarios are consistent with observational data on BJ's, as discussed in the main part of the paper and in more detail below. For storms having enhanced  $-CG$  activity, the increased rate at which negative charge is lowered to ground causes the storm to develop an average net positive

---

flashes almost always win this competition by virtue of the N and P regions being charged actively by the main storm current,  $I_1$ . (By contrast, the screening charge is derived from the passive screening current.) As conditions following each  $CG$  flash become increasingly favorable for an upward discharge, the way the discharge finally happens is by getting close enough to being triggered to win the competition during the post- $CG$  charging interval, rather than waiting to be produced immediately during a later  $CG$ . These features of the simulations are supported by the observational result that BJ's do not occur simultaneously with other discharges in the storm.

charge, thereby increasing the clear-air flow of negative screening charge to the cloud boundary. The equilibrium average positive charge would be such that the increased negative screening influx balances the average outflux due to the  $-CG$  discharges. Because of the exponential increase of clear-air electrical conductivity with altitude, most of the negative charge flow is to the upper cloud boundary. Blue jets provide an alternate way of balancing the negative  $CG$  outflux (equivalently, a positive charge influx), by transporting positive charge out of the upper cloud boundary. Similarly, negative blue jets would tend to be produced by inverted polarity storms following episodes of enhanced  $+CG$  activity.

As noted in a number of studies, storms have periods of increased cloud-to-ground lightning, both negative<sup>49, 50</sup> and positive<sup>34, 51</sup>. In this and previous studies<sup>52</sup>, model calculations indicate that the  $CG$  rate is controlled primarily by the amount of lower storm charge. For example, in Figs. S2 through S4,  $-CG$  discharges were initiated whenever the lower positive charge increased to  $\sim 15$ – $20$  C, more or less independent of the net storm charge and of the intracloud activity. This indicates that the rate at which  $-CG$ s occur depends primarily on the strength of the lower positive charging current  $I_2$  and leads to the inference or prediction that blue jets are favored in a storm when the lower positive charging increases. Such a situation would be expected when hail or graupel is being produced by a storm, due to reverse-polarity (positive) charging of hail during hail-ice crystal collisions<sup>8, 50, 52</sup>.

The prediction that blue jets would be preceded by  $CG$  discharges is consistent with the limited observational evidence of storms that produce such discharges. The studies by Wescott *et al.*<sup>53, 25</sup> found a statistical increase in the cumulative number of  $-CG$  discharges a few seconds prior to the occurrences of the blue jets and blue starters, followed by a decrease in the number of  $-CG$ s for a few seconds after the occurrences. The effect was most pronounced for blue jets but was also seen for blue starters. 10 out of 27 temporally isolated blue jets were found to have occurred within 1 s after a National Lightning Detection Network (NLDN)-indicated  $-CG$  discharge within 15 km of the jet<sup>25</sup>. An additional 11  $-CG$ s occurred 1 to 5 s prior to the jet occurrences. Analogous results were obtained for blue starters<sup>53</sup>. The reduction or apparent ‘lull’ in the  $-CG$  activity following the jets and starters would have reflected the time before the next  $-CG$  occurred. The starters and jets did not appear to be associated with particular lightning discharges, as most starters were found to ‘arise out of the anvil during a quiet (lightning) interval.’ However, the occurrence of  $-CG$  flashes prior to the upward discharges was considered possibly to be a ‘factor in creating the electric field configuration leading to the initiation of (the) blue starters and jets.’ The blue starters were found to be loosely concentrated near the centroid of the overall  $-CG$  activity, and also somewhat near the location of reported large hail.<sup>§</sup> In a later study<sup>23</sup>, a single blue jet was observed to occur within 4 s of a  $-CG$  discharge 14 km from the estimated location of the jet.

The recent report of a gigantic discharge over northeastern Mexico<sup>55</sup>, published while this paper was in review, shows a possible similar correlation with  $CG$  activity. The discharge occurred following a 4-minute increase in the NLDN-detected  $+CG$  rate in one of two storms that could have been the source of the event. The increase culminated in a 20-s ‘jump’ in the  $+CG$  rate, to

---

<sup>§</sup>We note that the jet-producing Arkansas storm system was similar to the June 11 STEPS storm<sup>54</sup> that produced the negative jet of Fig. 2, in that both produced severe winds and hail and developed above 15 km altitude in their convective cores. The STEPS storm and other storms like it<sup>19, 51, 56</sup> generally consist of a combination of inverted- and normal-polarity electrical structures, and produce both positive and negative  $CG$ s. The Arkansas storm may have been partially or substantially inverted as well, raising the question whether some of the Arkansas jets were like the STEPS jet and were negative rather than positive polarity.

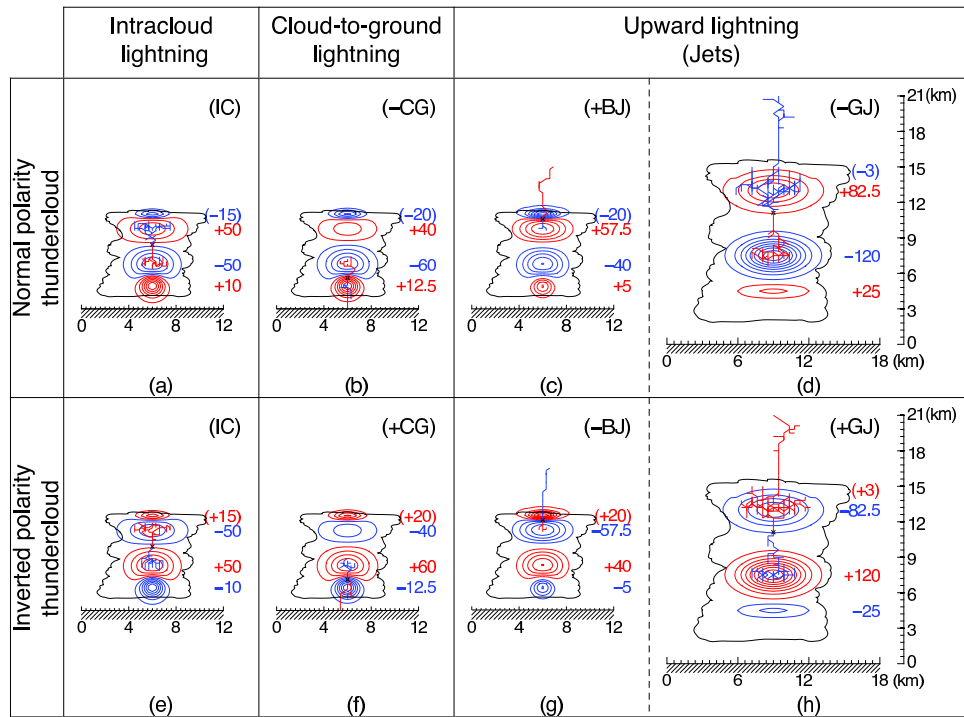


Figure S5: Illustrative lightning simulations for normal- and inverted-polarity storms, showing the four possible types of upward discharges, classified by initiation mechanism (blue jet and gigantic jet) and upward polarity (+ and -). Also shown for reference are the common forms of IC and CG flashes in normal and inverted storms. Blue jets will tend to be initiated by a precursor discharge (either CG or IC) that causes a charge imbalance in the storm.

one flash every 5 s, prior to the discharge's occurrence. The upward discharge was thought to be of negative polarity and to have originated in the upper negative charge of an inverted-polarity storm. If so it would have been a large blue jet-type discharge similar in its initiation mechanism to the STEPS jet of Fig. 2, but in a storm with a higher cloud top (~14 km above mean sea level).

We have classified upward discharges into two basic categories or types: 'blue' jets (BJs) and 'gigantic' jets (GJs). Heretofore, the two types have been distinguished primarily in terms of their maximum altitudes, and possibly their polarities, with blue jets (including blue starters) developing up to lower altitudes than gigantic jets, and appearing to transport positive charge upward, while gigantic jets transport negative charge upward. If it is assumed that the two types are produced by normally electrified storms, as the observational information has indicated, the present study indicates that the distinguishing characteristic between them is where they are initiated relative to the storm charges. The resulting breakdown scenarios give rise to positive blue jets (+BJs) and negative gigantic jets (-GJs).

In addition to the above, the observations of Fig. 2 show that negative upward jets can be produced by inverted polarity storms. We identify this as a negative blue jet (-BJ) based on where it was initiated relative to the storm charges. By extension, the inverted-storm analog of a -GJ would be a +GJ, with each polarity of GJ having as its source the main or mid-level charge of the storm. The four possible types of upward discharges are summarized in Fig. S5.

\*\*\*\*\*

Table S1: Heights and extents of charge regions for cylindrical disk model; storm of July 31, 1999 over Langmuir Laboratory (3 km MSL), and average charge values corresponding to the observed lightning rates.

Charge Layer	Altitude (km AGL <sup>a</sup> )	Altitude (km MSL <sup>b</sup> )	Depth (km)	Radius (km)	Avg. Charge (C)
Screening (SC)	8.00	11.00	0.5	4.0	−20
Upper Positive (P)	6.75	9.75	1.5	4.0	+60
Mid-level Negative (N)	3.75	6.75	1.5	3.0	−58
Lower Positive (LP)	2.00	5.00	1.5	1.5	+13

<sup>a</sup> AGL, above ground level; <sup>b</sup> MSL, above mean sea level

## References

1. Wescott, E. M., Sentman, D., Osborne, D., Hampton, D. & Heavner, M. Preliminary results from the Sprites94 aircraft campaign: 2. Blue jets. *Geophys. Res. Lett.* **22**(10), 1209–1212 (1995).
2. Boeck, W. L. *et al.* Observations of lightning in the stratosphere. *J. Geophys. Res.* **100**, 1465–1475 (1995).
3. Pasko, V. P., Stanley, M. A., Matthews, J. D., Inan, U. S. & Wood, T. G. Electrical discharge from a thundercloud top to the lower ionosphere. *Nature* **416**, 152–154 (2002).
4. Su, H. T. *et al.* Gigantic jets between a thundercloud and the ionosphere. *Nature* **423**, 974–976 (2003).
5. Rison, W., Thomas, R. J., Krehbiel, P. R., Hamlin, T. & Harlin, J. A GPS-based three-dimensional lightning mapping system: Initial observations in central New Mexico. *Geophys. Res. Lett.* **26**(23), 3573–3576 (1999).
6. Mathews, J. D., Stanley, M. A., Pasko, V. P., Wood, T. G., Inan, U. S., Heavner, M. J. & Cummer, S. A. Electromagnetic signatures of the Puerto Rico blue jet and its parent thunderstorm. *Eos Trans. AGU* **83**(47) (2002). Fall Meet. Suppl., Abstract A62D-02.
7. Krehbiel, P. R. *The electrical structure of thunderstorms*, in The Earth’s Electrical Environment, 90–113, Nat’l. Academy Press, Washington, D.C., 1986.
8. Williams, E. R. The tripolar structure of thunderstorms. *J. Geophys. Res.* **94**(D11), 13151–13167 (1989).
9. Kasemir, H. W. A contribution to the electrostatic theory of a lightning discharge. *J. Geophys. Res.* **65**(7), 1873–1878 (1960).
10. Mazur, V. & Ruhnke, L. H. Common physical processes in natural and artificially triggered lightning. *J. Geophys. Res.* **94**, 12913–12930 (1993).
11. Mazur, V. & Ruhnke, L. H. Model of electric charges in thunderstorms and associated lightning. *J. Geophys. Res.* **103**(D18), 23299–23308 (1998).



12. Coleman, L. M. *et al.* Effects of charge and electrostatic potential on lightning propagation. *J. Geophys. Res.* **108**(D9), 4298 (2003).
13. Raizer, Y. P., Milikh, G. M. & Shneider, M. N. On the mechanism of blue jet formation and propagation. *Geophys. Res. Lett.* **33**(23), L23801 (2006).
14. Marshall, T. C. *et al.* Observed electric fields associated with lightning initiation. *Geophys. Res. Lett.* **32**(3), L03813 (2005).
15. Wilson, C. T. R. Investigations on lightning discharges and on the electric field of thunderstorms. *Phil. Trans. Roy. Soc. Lond., A* **221**, 73–115 (1921).
16. Wilson, C. T. R. A theory of thundercloud electricity. *Proc. Roy. Soc. Lond., A* **236**, 297–317 (1956).
17. Rioussset, J. A., Pasko, V. P., Krehbiel, P. R., Thomas, R. J. & Rison, W. Three-dimensional fractal modeling of intracloud lightning discharge in a New Mexico thunderstorm and comparison with lightning mapping observations. *J. Geophys. Res.* **112**(D15203) (2007).
18. Lang, T. J. *et al.* The severe thunderstorm electrification and precipitation study. *Bull. Am. Meteorol. Soc.* **85**(8), 1107–1125 (2004).
19. Rust, W. D. *et al.* Inverted-polarity electrical structures in thunderstorms in the Severe Thunderstorm Electrification and Precipitation Study (STEPS). *Atmos. Res.* **76**(1–4), 247–271 (2005).
20. Behnke, S. A., Thomas, R. J., Krehbiel, P. R. & Rison, W. Initial leader velocities during intracloud lightning: Possible evidence for a runaway breakdown effect. *J. Geophys. Res.* **110**, D10207 (2005).
21. Lyons, W. A. *et al.* Upward electrical discharges from thunderstorm tops. *Bull. Am. Meteorol. Soc.* **84**(4), 445–454 (2003).
22. Pasko, V. P. & George, J. J. Three-dimensional modeling of blue jets and blue starters. *J. Geophys. Res.* **107**(A12), 1458 (2002).
23. Wescott, E. M., Stenbaek-Nielsen, H. C., Huet, P., Heavner, M. J. & Moudry, D. R. New evidence for the brightness and ionization of blue jets and blue starters. *J. Geophys. Res.* **106**(A10), 21549–21554 (2001).
24. Raizer, Y. P., Milikh, G. M. & Shneider, M. N. Leader–streamers nature of blue jets. *J. Atmos. Solar-Terr. Phys.* **69**(8), 925–938 (2007).
25. Wescott, E. M., Sentman, D. D., Heavner, M. J., Hampton, D. L. & Vaughan Jr., O. H. Blue jets: their relationship to lightning and very large hailfall, and their physical mechanisms for their production. *J. Atmos. Solar Terr. Phys.* **60**, 713–724 (1998).
26. Petrov, N. I. & Petrova, G. N. Physical mechanisms for the development of lightning discharges between a thundercloud and the ionosphere. *Tech. Phys.* **44**, 472–475 (1999).
27. Sukhorukov, A. I. & Stubbe, P. Problems of blue jet theories. *J. Atmos. Solar Terr. Phys.* **23**(13), 725–732 (1998).

28. Thomas, R. J. *et al.* Observations of VHF source powers radiated by lightning. *Geophys. Res. Lett.* **28**(1), 143–146 (2001).
29. Williams, E. R. *et al.* Lightning flashes conducive to the production and escape of gamma radiation to space. *J. Geophys. Res.* **111**, D16209 (2006).
30. Williams, E. R. Problems in lightning physics - the role of polarity asymmetry. *Plasma Sources Sci. & Tech.* **15**(2), S91-S108 (2006).
31. Krehbiel, P. R. *et al.* Thunderstorm charge studies using a simple cylindrical charge model, electric field measurements, and lightning mapping observations. *Eos Trans. AGU* **85**(47) (2004). Fall Meet. Suppl., Abstract AE23A-0843.
32. Thomas, R. J. *et al.* Accuracy of the Lightning Mapping Array. *J. Geophys. Res.* **109**, D14207 (2004).
33. Thomas, R. J. *et al.* New Mexico thunderstorms observed by the lightning mapping array, an overview of one season. *Eos Trans. AGU* **83**(47) (2002). Fall Meet. Suppl., Abstract A71B-0097.
34. Hamlin, T. D. The New Mexico Tech Lightning Mapping Array. Ph. D. Dissertation, New Mexico Inst. Mining & Tech., available at <http://hdl.handle.net/10136/40>, 164 pp., (2004).
35. Brown, K. A., Krehbiel, P. R., Moore, C. B. & Sargent, G. N. Electrical screening layers around electrified clouds. *J. Geophys. Res.* **76**, 2825-2835 (1971).
36. Marshall, T. C., McCarthy, M. P. & Rust, W. D. Electric field magnitudes and lightning initiation in thunderstorms. *J. Geophys. Res.* **100**, 7097-7103 (1995).
37. Stolzenburg, M. *et al.* Electric field values observed near lightning flash initiations. *Geophys. Res. Letts.* **34**, L04804, doi:10.1029/2006GL028777, (2007).
38. Gurevich, A. V. & Zybin, K. P. Runaway breakdown and electric discharges in thunderstorms. *Phys. Uspekhi* **44**, 1119-1140 (2001).
39. Krehbiel, P. R., Brook, M. & McCrory, R. A. An analysis of the charge structure of lightning discharges to ground. *J. Geophys. Res.* **84**, 2432-2456 (1979).
40. Krehbiel, P. R. An analysis of the electric field change produced by lightning. Ph. D. Dissertation, Univ. Manchester Inst. Sci. & Tech., available at <http://hdl.handle.net/10136/92>, 459 pp. (1981).
41. Uman, M. A. *The Lightning Discharge*. Acad. Press, 377 pp. (1987).
42. Krehbiel, P. R. On the initiation of upward lightning discharges above thunderstorms. *Eos Trans. AGU* **86**(18) (2005). Jt. Assem. Suppl., Abstract AE11A-05.
43. Pruppacher, H. R. & J. D. Klett *Microphysics of Clouds and Precipitation*. D. Reidel, Dordrecht, (1978).
44. Eack, K. B., Beasley, W. H., Rust, W. D., Marshall, T. C. & Stolzenberg, M. Initial results from simultaneous observation of X rays and electric fields in a thunderstorm. *J. Geophys. Res.* **101**, 29637-29640 (1996).

45. Dwyer, J. R. A fundamental limit on electric fields in air. *Geophys. Res. Letts.* **30**, 2055 doi:10.1029/2003GL017781 (2003).
46. Rust, W. D. & Moore, C. B. Electrical conditions near the bases of thunderclouds over New Mexico, *Quart. J. Roy. Met. Soc.* **100**, 450-468 (1974).
47. Sukhorukov, J. R., Mishin, E. V., Stubbe, P. & Rycroft, M. J. On blue jet dynamics. *Geophys. Res. Letts.* **23**, 1625-1628 (1996).
48. Tong, L., Nanbu, K. & Fukunishi, H. Randomly stepped model for upward electrical discharge from top of thundercloud. *J. Phys. Soc. Japan* **74**, 1093-1095 (2005).
49. Goodman, S. J. & MacGorman, D. R. Cloud-to-ground lightning activity in mesoscale convective complexes. *Mon. Weath. Rev.* **114**, 2320-2328 (1986).
50. Brown, R. A., Kaufman, C. A., & MacGorman, D. R. Cloud-to-ground lightning associated with the evolution of a multicell storm. *J. Geophys. Res.* **107**, 4397 (2002).
51. Weins, K. C., Rutledge, S. A. & Tessendorf, S. A. The 29 June 2000 supercell observed during STEPS. Part II: Lightning and charge structure. *J. Atmos. Sci.* **62**, 4151-4177 (2005).
52. Mansell, E. R., MacGorman, D. R., Ziegler, C. L., Straka, J. M. Charge structure and lightning sensitivity in a simulated multicell thunderstorm. *J. Geophys. Res.* **110**, D12101 (2005).
53. Wescott, E. M. *et al.* Blue starters: Brief upward discharges from an intense Arkansas thunderstorm. *Geophys. Res. Letts.* **23**, 2153-2156 (1996).
54. Lang, T. J. & Rutledge, S. A. Kinematic, microphysical, and electrical aspects of an asymmetric bow-echo mesoscale convective system observed during STEPS 2000. *J. Geophys. Res.* in press, (2008).
55. van der Velde, O. *et al.* Analysis of the first gigantic jet recorded over continental North America. *J. Geophys. Res.* **112**, D20104 (2007).
56. MacGorman, D. R. *et al.* TELEX: The Thunderstorm Electrification and Lightning Experiment. *Bull. Amer. Meteorol. Soc.* in press, (2008).